Journal of Andrology, Vol. 26, No. 2, March/April 2005

Stereological Quantification of Nerve Fibers Immunoreactive to PGP 9.5, NPY, and VIP in Rat Prostate During Postnatal Development

ROSARIO RODRÍGUEZ,* JOSÉ M. POZUELO,* ROCÍO MARTÍN,† RIÁNSARES ARRIAZU,* AND LUIS SANTAMARÍA‡§

*From the *Department of Physiology, Morphology, and Nutritional Sciences, San Pablo University, Madrid, Spain; †Service of Pathology, Hospital N Sra de Sonsoles, Ávila, Spain; and ‡Department of Morphology, School of Medicine, Autonomous University of Madrid, Madrid, Spain.*

ABSTRACT: This work was undertaken to study prostate innervation during the postnatal development of rats. It deals with the quantification of nervous fibers throughout all the regions of the rat prostate during the postnatal development using a general marker for nervous tissue, protein gene product 9.5, and 2 neuropeptides (NPY and VIP). Forty male Wistar rats (prepubertals, pubertals, young, and aged adults) were studied for immunohistochemistry of protein gene product (PGP 9.5), neuropeptide Y (NPY), and vasoactive intestinal polypeptide (VIP). They were also evaluated for length density of nerve fibers (L_V PGP 9.5, L_V NPY, L_V VIP). Nerve fibers immunoreactive to the 3 antigens studied were detected in all the groups and in all the prostate zones. Periductal L_V NPY evidenced a significant increase in the pubertal group, maintained throughout adult life. Periductal L_V VIP showed a significant increase in young adults. The length densities of VIP and NPY fibers were significantly higher in periductal and ampular locations in comparison with dorsal and ventral sites. It can be concluded that the relative amount of nerve fibers in rat prostate, detected by PGP 9.5, does not change during postnatal development. There were significant changes in NPY and VIP fibers, showing an increase in periurethral ducts at puberty. The abundance of peptidergic innervation around the excretory ducts is related to their contractility. The development of innervation of periurethral ducts is regulated by androgens.

Key words: Innervation, neuropeptides.

J Androl 2005;26:197–204

The autonomous nervous system is relevant in the maintenance of structural and functional integrity of the prostate (Hedlund et al, 1996; Hedlund et al, 1997). Thus, prostatic denervation leads to an extensive atrophy of the rat prostate (Wang et al, 1991; Luján et al, 1998). Besides the catecholaminergic and cholinergic innervation, a wide variety of peptidergic fibers have been described in the prostate gland, such as neuropeptide Y (NPY), vasoactive intestinal polypeptide (VIP), substance P (SP), calcitonin gene-related peptide (CGRP) nerves, etc (Adrian et al, 1984; Vaalasti et al, 1986; Crowe et al, 1987; Higgins and Gosling, 1989; Crowe et al, 1991). It seems that neuropeptides might be implicated in the physiology of the prostate (Dixon et al, 2000; Ventura et al, 2002).

Nevertheless, the role of peptidergic innervation in prostate function is not yet well ascertained. The regulatory peptides contained in the autonomic terminals could intervene in the prostatic secretion (Gkonos et al, 1995) but also in the development and growth of the prostate acini, modulating the action of androgens (Chapple et al, 1991). Some neuropeptides such as VIP might be implicated in the epithelial proliferation of prostatic acini (Juarranz et al, 2001), and several investigations are relating peptidergic innervation and neuroepithelial interactions with prostatic pathologies such as cancer or benign prostate hyperplasia (Martín et al, 2000; Cornell et al, 2003).

The rat has frequently been employed as an experimental model to study the biology and pathology of the prostate (Price, 1963; Angelsen et al, 1999); therefore, it seems interesting to investigate the nature and distribution of peptidergic nerves during the postnatal development of rat prostate. Thus, the aims of this work are 1) to study the presence, distribution, and quantification of nervous fibers throughout all the regions of the rat prostate during the postnatal development using a general marker for nervous tissue, protein gene product 9.5 (PGP 9.5); and 2) to study the presence, distribution, and quantification of peptidergic innervation throughout all the regions of the rat prostate during the postnatal development using 2 neuropeptides (NPY and VIP). These studies will be performed combining immunohistochemistry and stereologic nonbiased methods for quantification of length of nerve fibers.

Correspondence to: Luis Santamaría, Department of Morphology, School of Medicine, Autonomous University, C/ Arzobispo Morcillo, 2, E-28029 Madrid, Spain (e-mail: luis.santamaria@uam.es).

Received for publication July 7, 2004; accepted for publication October 14, 2004.

Materials and Methods

Animals

The study was carried out on 40 Wistar male rats. The animals were placed in 4 groups (10 rats per group) according to postnatal development: prepubertal (15 days old), pubertal (30 days old), young adult (90 days old), and old adult (540 days old). Animal protocols agreed with the guidelines for the care and use of research animals adopted by the Society for the Study of Reproduction. All rats were killed by exsanguination after CO_2 narcosis. The prostate complex was dissected from the abdominal cavity of each animal and later exhaustively cut into 2-mm-wide slices. The section plane was perpendicular to the sagittal axis of the gland. All specimens were fixed by immersion in 10% paraformaldehyde in phosphate-buffered saline (PBS) pH 7.4 during 24 hours and then embedded in paraffin.

Sampling Procedure

For each prostate, all slices obtained were embedded in a paraffin block. The blocks were then serially sectioned. Five-μm-thick sections (for immunohistochemistry and routine hematoxylin and eosin techniques) alternating with 10-μm-thick sections (for stereological methods) were performed for each block. Both dorsal and ventral prostate regions were included in every section.

For the evaluation of immunohistochemical and stereological studies, 20 sections were selected by random systematic sampling (Gundersen and Osterby, 1981; Gundersen, 1986) from each block obtained from each animal.

Immunohistochemistry

Nerve fibers immunoreactive to PGP 9.5, NPY, and VIP were studied in all the regions of the rat prostate (dorsal, ampular, and ventral) from pubertal, young, and aging adults. As in prepubertal animals, the morphologic identification of the prostate regions was impossible; all the immunohistochemical and quantitative studies were performed in the prepubertal prostate gland considered as a whole. However, the compartment of excretory ducts was easily identified throughout all the age groups and then separately evaluated in all the groups.

The nerve fibers immunoreactive for each of the markers employed were evaluated in the periglandular compartment from dorsal, ampular, and ventral prostate. The periglandular zone was defined as a band 10-μm wide around the acini. To evaluate the ductal innervation, a periductal zone with an extension of 20 μm (including the periductal muscular layer) around the excretory ducts was also considered. The remaining stroma, excluding the periglandular or periductal zone, was named ''interglandular compartment'' and was not considered in order to perform quantitative evaluation.

At least 3 selected slides per animal (per prostate) and per antigen were immunostained in all the animal groups. Deparaffinized and rehydrated tissue sections were treated for 30 minutes with hydrogen peroxide 0.3% in PBS pH 7.4 to block endogenous peroxidase. To detect PGP 9.5 immunoreactivity, sections were incubated with a monoclonal anti-PGP 9.5 antibody (Biomeda, Foster City, Calif) at a dilution of 1:25. To detect NPY and VIP immunoreactivities, sections were incubated, respectively, with a polyclonal anti-NPY antibody (Hammersmith Hospital, London, United Kingdom) at a dilution of 1:1000 and with a polyclonal anti-VIP antibody (Biomeda) at a dilution of 1:2. All incubations with primary antisera were diluted in PBS pH 7.4 containing 1% bovine serum albumin (BSA) plus 0.1% sodium azide. All incubations with primary antisera were left overnight at 4ºC.

The second antibody used for primary monoclonal antibodies was a biotin–caproyl–anti-mouse immunoglobulin (Biomeda). The second antibody used for primary polyclonal antibodies was a biotin–caproyl–anti-rabbit immunoglobulin (Biomeda). Both were diluted at 1:400 in PBS containing 1% BSA without sodium azide. The tissues were incubated for 30 minutes at room temperature. Thereafter, sections were incubated with a streptavidin-biotin-peroxidase complex (Biomeda). The immunostaining reaction product was developed using 0.1 g diaminobenzidine (DAB) (3,3′,4,4′–tetraminobiphenyl; Sigma, St Louis, Mo) in PBS (200 mL) plus 40 μL hydrogen peroxide.

After immunoreactions, sections were counterstained with methyl green. All slides were dehydrated in ethanol and mounted in a synthetic resin (Depex; Serva, Heidelberg, Germany).

The specificity of the immunohistochemical procedures was checked by incubation of sections with nonimmune serum instead of the primary antibody.

Stereological Methods

Length fiber density (length of fiber per unit of volume of reference space: L_V) was evaluated for each age group in each prostate region and tissular compartment defined above and for every immunohistochemical type. The reference space was considered as the stromal and epithelial components together. Briefly, the procedure used was as follows. Three 10-μm-thick PGP 9.5–, NPY-, and VIP-immunostained sections per animal (per prostate) were chosen by systematic random sampling. For all practical purposes, biological microstructures such as capillaries, tubules, and axons can be regarded as linear features. The most important stereological attribute of linear features is their L_V, that is, total line length per unit volume from which absolute length can be calculated, provided the reference volume is known (Mayhew, 1991). A nerve profile was defined as a portion of nerve segment seen regardless of its size and length. The isotropic distribution of the nerve fibers was assumed in this study (Howard and Reed, 1998).

An average of 100 fields per section in each prostate zone were systematically randomly sampled and used to count the number of immunoreactive nerve profiles. All measurements were performed using an Olympus microscope with 100× objective (numerical aperture 1.4) at a final magnification of 1200×. The microscope was connected to a videocamera and supplied with a motorized stage connected to a computer. The software used (Stereologic Software Package, CAST-GRID; Interactivision, Silkeborg, Denmark) (Martín et al, 1997) controls the XY movement of the stage and allows the automatic selection of microscopic fields. The program generates a disector grid that is superimposed onto the microscopic image captured by the videocamera and projected onto the monitor.

The nerve profiles eligible for counting were those sampled by the disector frame and fulfilling the Sterio rule (Howard and Reed, 1998). They were designed as Q^-.

The L_V was calculated by the following formula:

$$L_V = (2 \times \Sigma Q^-)/\Sigma A$$

where Q^- = number of immunopositive nerve profiles and ΣA = total area sampled, that is, area of disector frame (1312 μm^2) multiplied by the number of selected fields.

Statistical Evaluations

Data were adjusted to a normal population distribution by logarithmic transformation before statistical analysis. For each parameter studied, the mean ± SD was calculated. The differences among prostate zones for each age group and the differences among age groups for each prostate zone and tissular compartment were evaluated by analysis of variance (ANOVA). Comparison between each pair of means was performed using the Student Newman-Keuls test. The level of significance chosen was *P* less than .05.

Results

Immunohistochemical Findings

PGP 9.5–immunoreactive nerves were observed for each age group, in each prostate region, including postganglionic neurons from ganglia associated to periprostatic capsule (Figures 1a and b), and periglandular or interglandular compartments (Figures 1c and d). The interglandular plexus was evident in all the groups (Figures 1c and d). NPY-immunoreactive nerves were observed from the postnatal period in each prostate region and tissular compartment (Figure 1e). NPY fibers from the periductal compartment were more notable in both pubertal and adult rats (Figures 1f and g). Immunoreactivity to VIP was already detected in periglandular and interglandular nerves in prepubertal rats (Figure 1h) and also in clusters of periprostatic neurons and in nerve bundles from prepubertal and pubertal animals (Figure 1i). VIP immunostaining in periglandular fibers was evident throughout the postpubertal development (Figures 1j and k). Neuronal, fascicular, and periglandular immunoreactivity to VIP was remarkable in aging animals (Figure 1k through m).

Stereological Quantification

Comparison of the Estimates of Length Density of Fibers Among Groups of Age—L_V PGP 9.5 did not show significant differences among age groups in all the tissular compartments evaluated (periglandular and periductal) (Figure 2). L_V NPY from the periglandular compartment showed a significant decrease in both young and old adults in comparison with the pubertal and prepubertal animals (Figure 3). Conversely, L_V NPY from the periductal compartment evidenced a significant increase in the pubertal group, maintained throughout adult life; these findings are expressed in Figure 3. The length density for VIP nerve fibers did not show significant differences among age groups in periglandular compartment (Figure 4), whereas L_V VIP from periductal structures showed a significant increase in young adults in relation to prepubertal and pubertal animals, and no changes were observed in L_V VIP between young and aged groups (Figure 4).

Comparison of the Estimates of Length Density of Fibers Among Prostate Regions—When the length density of nerve fibers was compared among prostate regions, the following results were observed:

Periglandular L_V PGP 9.5 did not show significant differences among regions in the pubertal group (Figure 5), whereas in both young and aging adult rats the L_V PGP 9.5 was significantly greater in the periductal localization than in the periglandular compartment of ampular, dorsal, and ventral regions (Figure 5).

Concerning the periglandular L_V NPY, no changes among regions were observed in pubertal animals (Figure 6), whereas in both young and aging adult groups the length density of NPY nerve fibers was significantly increased in the periductal compartment in comparison with the ampular, dorsal, and ventral zones (Figure 6).

The periglandular length density of VIP fibers from pubertal rats shows a significant increase in both ductal and ampular regions with relation to dorsal and ventral prostate (Figure 7), whereas in adult (young and aging) rats the increase of L_V VIP was significant only in the ducts (Figure 7).

Discussion

The length density of PGP 9.5–immunoreactive fibers (ie, length of nerve fibers per unit of volume) remains unchanged during the postnatal development. Therefore, the relative amount of nerve fibers, independent of the type of innervation, was constant in the prostate throughout the postnatal life of the rat. However, within this global population of nerve fibers, changes in the density of fibers immunoreactive to some neuropeptides (VIP, NPY) in relation to the pubertal outcome have been observed. These changes were evident at the level of excretory ducts and consisted of an increase of NPY- and VIP-immunostained fibers. It seems that changes in density of VIP and NPY fibers are mostly related to increased synthesis. These neuropeptides probably modulate the androgen action on prostate epithelial cells (Gkonos et al, 1995); therefore, its synthesis probably changes in relation to the situation of androgenic function during prostate development. These findings agree with other studies in the urogenital tract from rats (Properzi et al, 1992) or in sexual accessory glands from hamsters (Chow et al, 1997). The abundance of peptidergic innervation around the excretory ducts is related to the modulation of contractility of the

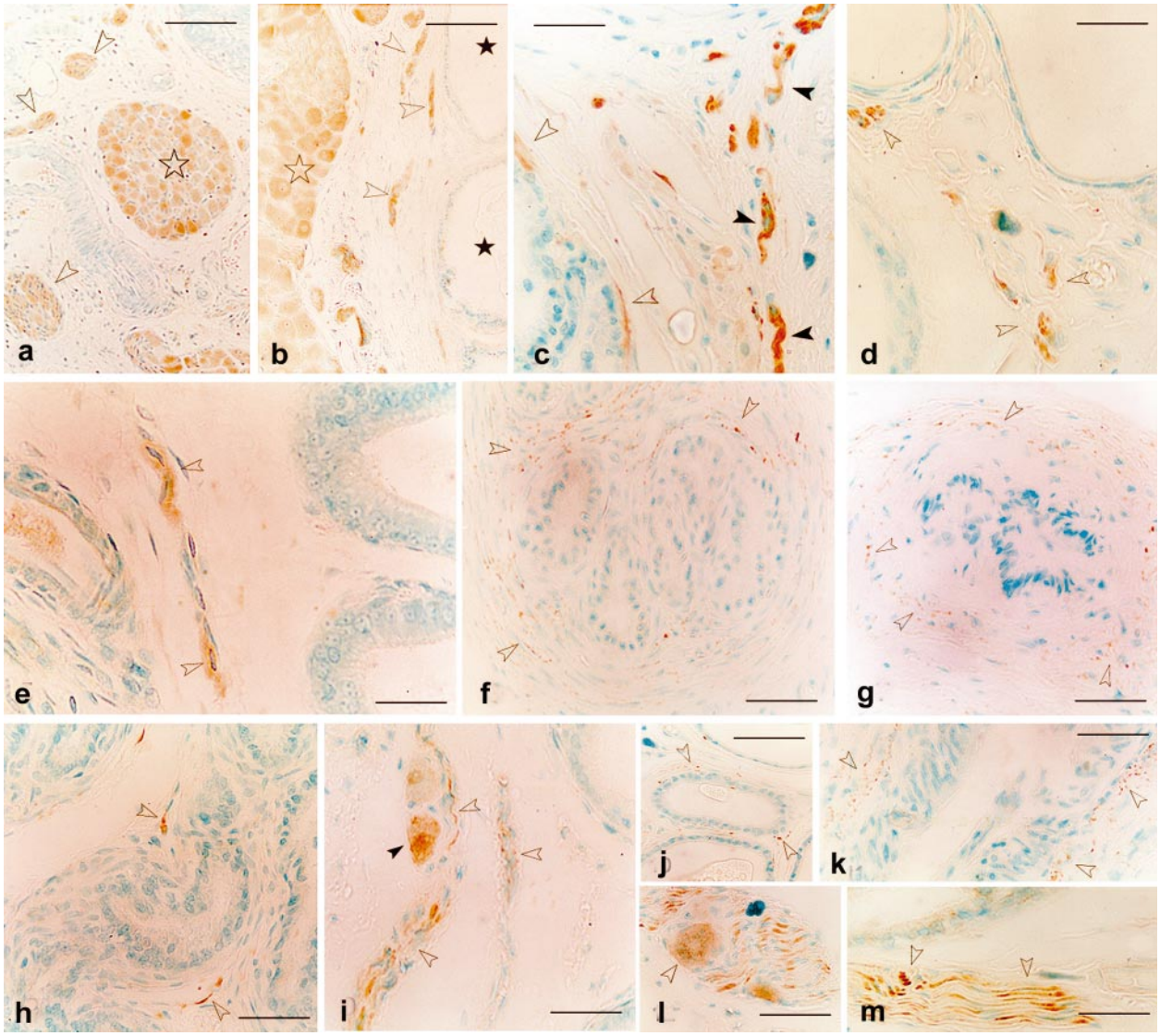

Figure 1. **(a)** Periprostatic autonomic ganglion (star) from a prepubertal rat. The neurons show immunoreactivity to PGP 9.5. Some immunoreactive nerve bundles are also seen (arrowheads). Immunostaining to PGP 9.5. Scale bar = 190 μm. **(b)** Periprostatic autonomic ganglion (star) from a pubertal rat. The neurons show immunoreactivity to PGP 9.5. Some immunoreactive nerve bundles are seen (arrowheads). Several acini from ampular region are observed (black stars). Immunostaining to PGP 9.5. Scale bar = 110 μm. **(c)** Periglandular (arrowheads) and interglandular (black arrowheads) nerve fibers immunoreactive to PGP 9.5. Dorsal prostate from a young adult. Immunostaining to PGP 9.5. Scale bar = 60 μm. **(d)** Interglandular (arrowheads) nerve fibers immunoreactive to PGP 9.5. Ventral prostate from an aged adult. Immunostaining to PGP 9.5. Scale bar = 60 μm. **(e)** NPY-immunoreactive fibers (arrowheads) in the interglandular compartment of a prepubertal rat prostate. Immunostaining to NPY. Scale bar = 60 μm. **(f)** NPY-immunoreactive neuroendings (arrowheads) in the periductal compartment of periurethral ducts from a pubertal rat prostate. Immunostaining to NPY. Scale bar = 60 μm. **(g)** NPY-immunoreactive neuroendings (arrowheads) in the periductal compartment of periurethral ducts from a young adult rat prostate. Immunostaining to NPY. Scale bar = 60 μm. **(h)** VIP-immunoreactive fibers (arrowheads) in the interglandular compartment of a prepubertal rat prostate. Immunostaining to VIP. Scale bar = 60 μm. **(i)** Periprostatic autonomic ganglion (black arrowhead) from a pubertal rat. One neuron shows VIP immunoreactivity. Some immunoreactive nerve bundles are also seen (arrowheads). Immunostaining to VIP. Scale bar = 60 μm. **(j)** VIP-immunoreactive neuroendings (arrowheads) in the periglandular compartment of ampular acini from a young adult rat prostate. Immunostaining to VIP. Scale bar = 90 μm. **(k)** VIP-immunoreactive neuroendings (arrowheads) in the periductal compartment of periurethral ducts from an aged adult rat prostate. Immunostaining to VIP. Scale bar = 60 μm. **(l)** Periprostatic autonomic ganglion from an aged rat. One neuron shows VIP immunoreactivity (arrowhead). Some immunoreactive nerve fibers are also seen. Immunostaining to VIP. Scale bar = 60 μm. **(m)** VIP-immunoreactive fibers (arrowheads) in the interglandular compartment of an aged rat prostate. Immunostaining to VIP. Scale bar = 60 μm.

ductal wall (Pennefather et al, 2000; Ventura et al, 2002) necessary for the excretion of prostate fluid during ejaculation (Iwata et al, 2001). In this sense, the particular abundance of innervation in prostate ducts might be associated with the exclusive presence of serotoninergic neuroendocrine cells among the columnar cells from periurethral ducts and their possible role in regulating the excretion of prostatic fluid toward the urethra (Rodríguez

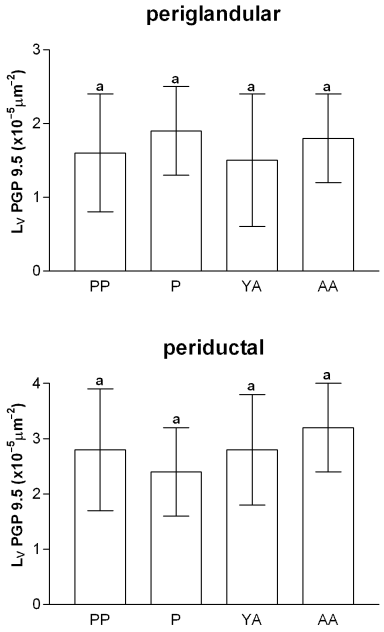

Figure 2. Comparison of length density of nerve fibers (L_V) of PGP 9.5–immunostained nerves expressed $\times 10^{-5}$ µm^{-2}, after logarithmic transformation, among age groups PP (prepubertals), P (pubertals), YA (young adults), and AA (aged adults) for periglandular and periductal compartments. In each graph, the letters over each error bar indicate the significance: Bars affected by different letters show significant differences ($P < .05$).

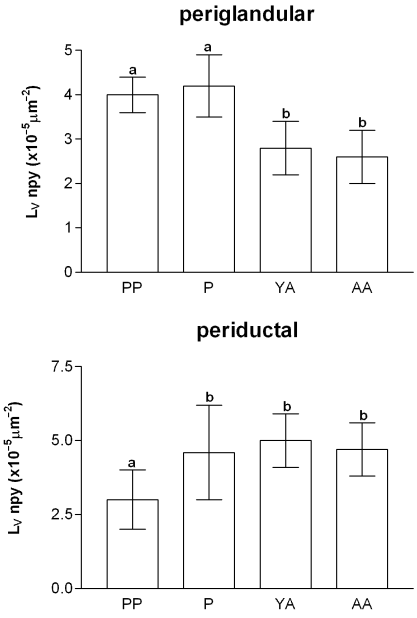

Figure 3. Comparison of length density of nerve fibers (L_V) of NPY-immunostained nerves expressed $\times 10^{-5}$ µm^{-2}, after logarithmic transformation, among age groups PP (prepubertals), P (pubertals), YA (young adults), and AA (aged adults) for periglandular and periductal compartments. In each graph, the letters over each error bar indicate the significance: Bars affected by different letters show significant differences ($P < .05$).

et al, 2003). The parallelism between the increase of neuroendocrine cells and both NPY- and VIP-immunoreactive fibers, after or around puberty, suggesting an androgenic effect on development of prostate innervation was also found interesting (Rodríguez et al, 2003).

The periglandular compartment of the ampular gland was the zone most densely populated by VIP-immunoreactive nerve fibers. The presence of these subepithelial nerves in the ampular acini suggests a role for the VIP in the regulation of their secretory activity (Juarranz et al, 2001; Ventura et al, 2002). This agrees with the detection of vipergic receptors in the epithelium of rat prostate (Carmena et al, 1985; Carmena et al, 1986a; Carmena et al, 1986b; Carmena et al, 1988).

It was interesting to note the decrease of L_V NPY in the periglandular compartment after puberty. Age-dependent reduction of prostatic autonomic innervation was indicated almost 50 years ago (Casas, 1958), and age-related diminution in peripheral autonomic innervation has previously been described in several organs; that is, the aging rat has a reduced sympathetic supply to the urinary tract (Warburton and Santer, 1994). One possible cause of such a reduction is the depletion of detectable neuropeptides, because neurons may become less active (Cowen, 1993). Other authors (Properzi et al, 1992) have also observed an increase of NPY-immunoreactive fibers in pubertal rat prostate, but these findings were maintained dur-

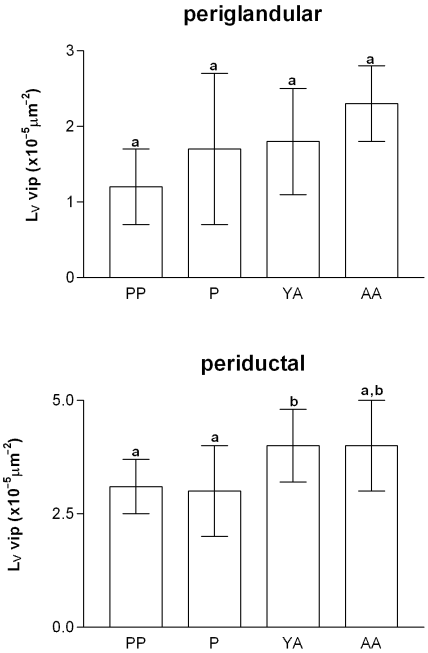

Figure 4. Comparison of length density of nerve fibers (L_V) of VIP-immunostained nerves expressed $\times 10^{-5}$ µm^{-2}, after logarithmic transformation, among age groups PP (prepubertals), P (pubertals), YA (young adults), and AA (aged adults) for periglandular and periductal compartments. In each graph, the letters over each error bar indicate the significance: Bars affected by different letters show significant differences ($P < .05$).

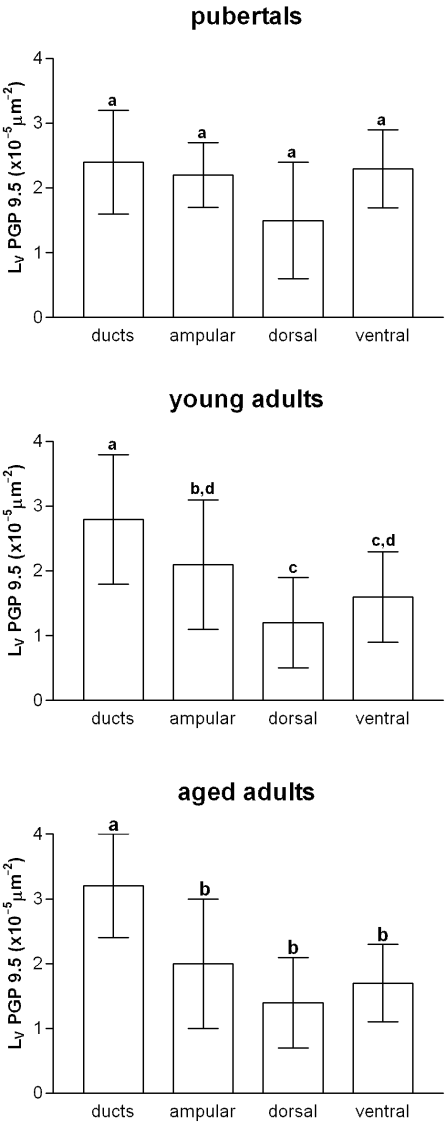

Figure 5. Comparison of length density of PGP 9.5–immunostained nerves (L_V PGP 9.5) expressed $\times 10^{-5}$ µm^{-2}, after logarithmic transformation, among prostate regions (ducts, ampular, dorsal, and ventral) for pubertals, young adults, and aged adults. In each graph, the letters over each error bar indicate the significance: Bars affected by different letters show significant differences ($P < .05$).

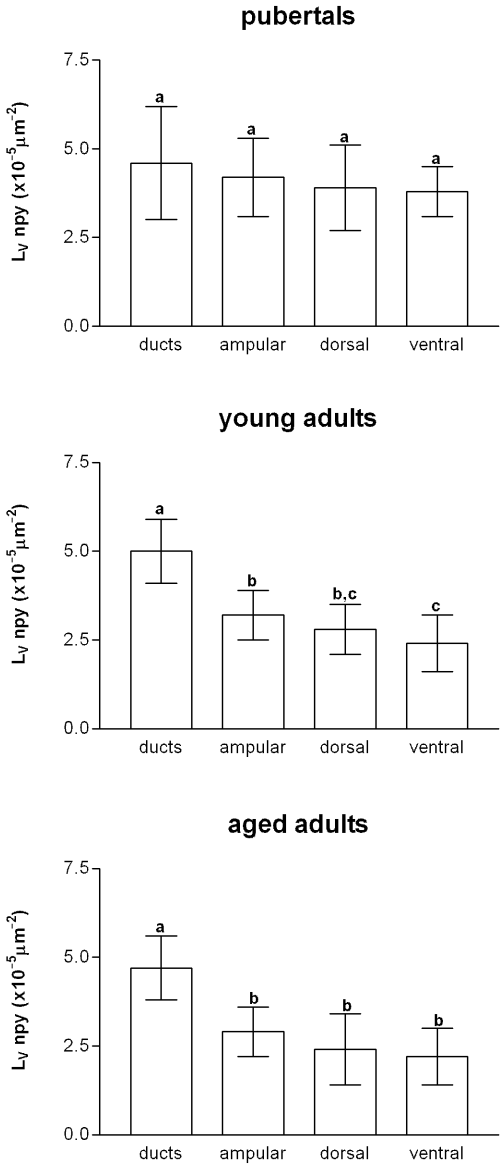

Figure 6. Comparison of length density of NPY-immunostained nerves (L_V NPY) expressed $\times 10^{-5}$ µm^{-2}, after logarithmic transformation, among prostate regions (ducts, ampular, dorsal, and ventral) for pubertals, young adults, and aged adults. In each graph, the letters over each error bar indicate the significance: Bars affected by different letters show significant differences ($P < .05$).

ing adult life. This discordance with the present results might be attributed to an absence of rigorous quantification, because other authors (Chow et al, 1997), using stereological nonbiased methods for evaluation of the NPY innervation in the prostate of hamster, agree with the results of this study.

The next conclusions can be made: 1) The relative amount of global nerve fibers in rat prostate, detected by PGP 9.5, does not change during postnatal development. Nevertheless, there were significant changes in the NPY and VIP subpopulations of nerve fibers, detecting their increase in periurethral ducts in the pubertal stage. 2) The abundance of peptidergic innervation around the excretory ducts might be related to the modulation of contractility of ductal wall necessary for the excretion of prostate secretions during ejaculation. 3) The periglandular compartment from the ampular prostate was the most densely innervated in comparison with dorsal and ventral prostate, which might be related to the abundance of smooth muscle in the ampular region. 4) The parallelism between the increase of neuroendocrine cells and both NPY- and VIP-immunoreactive fibers, after or around puberty, suggests

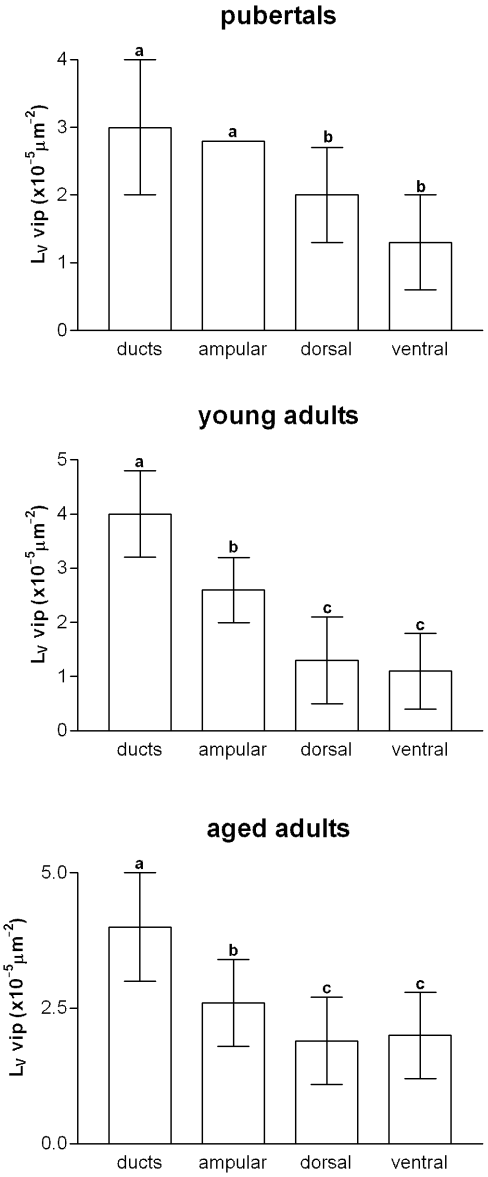

Figure 7. Comparison of length density of VIP-immunostained nerves (L_V VIP) expressed $\times 10^{-5}$ μm^{-2}, after logarithmic transformation, among prostate regions (ducts, ampular, dorsal, and ventral) for pubertals, young adults, and aged adults. In each graph, the letters over each error bar indicate the significance: Bars affected by different letters show significant differences ($P < .05$).

an androgenic effect on the development of innervation of periurethral ducts in rat prostate.

References

Adrian TE, Gu J, Allen JM, Tatemoto K, Polak JM, Bloom SR. Neuropeptide Y in the human male genital tract. *Life Sci.* 1984;35:2643–2648.

Angelsen A, Falkmer S, Sandvik AK, Waldum HL. Pre- and postnatal testosterone administration induces proliferative epithelial lesions with neuroendocrine differentiation in the dorsal lobe of the rat prostate. *Prostate.* 1999;40:65–75.

Carmena MJ, Prieto JC. Cyclic AMP response to vasoactive intestinal peptide and beta-adrenergic or cholinergic agonists in isolated epithelial cells of rat ventral prostate. *Biosci Rep.* 1985;5:791–797.

Carmena MJ, Recio MN, Prieto JC. Influence of castration and testosterone treatment on the vasoactive intestinal peptide receptor/effector system in rat prostatic epithelial cells. *Biochim Biophys Acta.* 1988; 969:86–90.

Carmena MJ, Sancho JI, Prieto JC. Additive effect of VIP or isoproterenol on forskolin-stimulated cyclic AMP accumulation in rat prostatic epithelial cells. *Biochem Int.* 1986a;13:479–485.

Carmena MJ, Sancho JI, Prieto JC. Effects of age and androgens upon functional vasoactive intestinal peptide receptors in rat prostatic epithelial cells. *Biochim Biophys Acta.* 1986b;888:338–343.

Casas AP. The innervation of the human prostate. *Z Mikrosk Anat Forsch.* 1958;64:608–633.

Chapple CR, Crowe R, Gilpin SA, Gosling J, Burnstock G. The innervation of the human prostate gland—the changes associated with benign enlargement. *J Urol.* 1991;146:1637–1644.

Chow PH, Dockery P, Cheung A. Innervation of accessory sex glands in the adult male golden hamster and quantitative changes of nerve densities with age. *Andrologia.* 1997;29:331–342.

Cornell RJ, Rowley D, Wheeler T, Ali N, Ayala G. Neuroepithelial interactions in prostate cancer are enhanced in the presence of prostatic stroma. *Urology.* 2003;4:870–875.

Cowen T. Aging and the autonomic nervous system: a result of nerve-target interactions? A review. *Mech Aging Dev.* 1993;68:163–173.

Crowe R, Chapple CR, Burnstock G. The human prostate gland: a histochemical and immunohistochemical study of neuropeptides, serotonin, dopamine beta-hydroxylase and acetylcholinesterase in autonomic nerves and ganglia. *Br J Urol.* 1991;68:53–61.

Crowe R, Milner P, Lincoln J, Burnstock G. Histochemical and biochemical investigation of adrenergic, cholinergic and peptidergic innervation of the rat ventral prostate 8 weeks after streptozotocin-induced diabetes. *J Auton Nerv Syst.* 1987;20:103–112.

Dixon JS, Jen PY, Gosling JA. The distribution of vesicular acetylcholine transporter in the human male genitourinary organs and its co-localization with neuropeptide Y and nitric oxide synthase. *Neurourol Urodyn.* 2000;19:185–194.

Gkonos J, Kongrad A, Roos B. Neuroendocrine peptides in the prostate. *Urol Res.* 1995;23:81–87.

Gundersen HJ, Osterby R. Optimizing sampling efficiency of stereological studies in biology: or ''do more less well!''. *J Microsc.* 1981; 121:65–73.

Gundersen HJ. Stereology of arbitrary particles. A review of unbiased number and size estimations and the presentation of some new ones in memory of William R. Thompson. *J Microsc.* 1986;143:3–45.

Hedlund P, Ekstrom P, Larsson B, Alm P, Andersson KE. Heme oxygenase and NO-synthase in the human prostate-relation to adrenergic, cholinergic and peptide-containing nerves. *J Auton Nerv Syst.* 1997; 63:115–126.

Hedlund P, Larsson B, Alm P, Andersson KE. Nitric oxide synthase-containing nerves and ganglia in the dog prostate: a comparison with other transmitters. *Histochem J.* 1996;28:635–642.

Higgins JR, Gosling JA. Studies on the structure and intrinsic innervation of the normal human prostate. *Prostate Suppl.* 1989;2:5–16.

Howard CV, Reed MG. Length estimation. In: Howard CV, Reed MG, eds. *Unbiased Stereology. Three-Dimensional Measurement in Microscopy.* Oxford, United Kingdom: Bios Scientific Publishers; 1998: 125–128.

Iwata T, Ukimura O, Inaba M, Kojima M, Kumamoto K, Ozawa H, Kawata M, Miki T. Immunohistochemical studies on the distribution of nerve fibers in the human prostate with special reference to the anterior fibromuscular stroma. *Prostate.* 2001;48:242–247.

Juarranz MG, Bodega G, Prieto JC, Guijarro LG. Vasoactive intestinal

peptide (VIP) stimulates rat prostatic epithelial cell proliferation. *Prostate.* 2001;47:285–292.

Luján M, Páez A, Llanes L, Angulo J, Berenguer A. Role of autonomic innervation in rat prostatic structure maintenance: a morfometric analysis. *J Urol.* 1998;160:1919–1923.

Martín R, Fraile B, Peinado F, et al. Immunohistochemical localization of protein gene product 9.5, ubiquitin, and neuropeptide Y immunoreactivities in epithelial and neuroendocrine cells from normal and hyperplastic human prostate. *J Histochem Cytochem.* 2000;48:1121–1130.

Martín R, Nieto S, Santamaría L. Stereologic estimates of volume-weighted mean nuclear volume in colorectal adenocarcinoma: correlation with histologic grading, Dukes' staging cell proliferation activity and p53 protein expression. *Gen Diagn Pathol.* 1997;143:29–38.

Mayhew TM. The new stereological methods for interpreting functional morphology from slices of cells and organs. *Exp Physiol.* 1991;76:663–665.

Pennefather JN, Lau WA, Mitchelson F, Ventura S. The autonomic and sensory innervation of the smooth muscle of the prostate gland: a review of pharmacological and histological studies. *J Auton Pharmacol.* 2000;20:193–206.

Price D. Biology and the prostate and related tissues. *NCI Monogr.* 1963;12:1–28.

Properzi G, Cordeschi G, Francavilla S. Postnatal development and distribution of peptide-containing nerves in the genital system of the male rat. An immunohistochemical study. *Histochemistry.* 1992;97:61–68.

Rodríguez R, Pozuelo JM, Martín R, Henriques-Gil N, Haro M, Arriazu R, Santamaría L. Presence of neuroendocrine cells during postnatal development in rat prostate: immunohistochemical, molecular, and quantitative study. *Prostate.* 2003;57:176–185.

Vaalasti A, Tainio H, Pelto HM, Hervonen A. Light and electron microscope demonstration of VIP- and enkephalin-immunoreactive nerves in the human male genitourinary tract. *Anat Rec.* 1986;215:21–27.

Ventura S, Pennefather J, Mitchelson F. Cholinergic innervation and function in the prostate gland. *Pharmacol Ther.* 2002;94:93–112.

Wang JM, Mc Vary KT, Chung L. Requirement of innervation for maintenance of structural and functional integrity in the rat prostate. *Biol Reprod.* 1991;44:1171–1176.

Warburton AL, Santer RM. Sympathetic and sensory innervation of the urinary tract in young adult and aged rats: a semi-quantitative histochemical and immunohistochemical study. *Histochem J.* 1994;26:127–133.